



Düzce University Journal of Science & Technology

Research Article

Sequentially Modified Gravitational Search Algorithm for Image Enhancement

 Ferzan KATIRCIOĞLU ^{a,*},  Uğur GÜVENÇ ^b

^a Department of Control and Automation, Duzce VHS, Düzce University, Düzce, TURKEY

^b Electrical-Electronics Engineering, Faculty of Technology, Düzce University, Düzce, TURKEY

* Corresponding author's e-mail address: ferzankatircioglu@duzce.edu.tr

DOI: 10.29130/dubited.710153

ABSTRACT

Gravitational Search Algorithm (GSA) is based on the acceleration trend feature of objects with a mass towards each other and includes many interdependent parameters. The gravitational constant among these parameters influences the speeds and positions of the agents, meaning that the search capability depends on the largescale gravitational constant. The proposed new algorithm, which was obtained with the use of two operators at different times of the call and sequentially doing works, was named as Sequentially Modified Gravitational Search Algorithm (SMGSA). SMGSA is applied to 10 basic and 6 composite benchmark functions. Each function is run 30 times and the best, mean and median values are obtained. The achieved results are compared with the Genetic Algorithm (GA), Particle Swarm Optimization (PSO) and GSA among the heuristic optimization algorithms. Between GSA and the operator for each function convergence speed, standard deviation and graphical comparisons are included. Beside this, by using the Wilcoxon signed rank test, the comparison of the averages of the data as two dependent groups of GSA and the new operators is performed. It is seen that the obtained results provided better results than the other methods. Additionally, in this study, SMGSA was applied to the transformation function among image enhancement techniques which are engineering applications. The success of this method has been increased by optimizing the parameters of the transformation function used. Effective improvement has been achieved in terms of both visual and information quality.

Keywords: Gravitational Search Algorithm, Optimization, Image Enhancement.

Görüntü İyileştirme için Sıralı Modifiyeli Yerçekimi Arama Algoritması

ÖZET

Yerçekimi Arama Algoritması (GSA), kütlesi birbirine yakın olan nesnelerin hızlanma eğilimi özelliğini temel almakta olup, birbirine bağlı birçok parametre içermektedir. Bu parametreler arasındaki yerçekimi sabiti ajanların hızlarını ve konumlarını etkiler, yani arama kabiliyeti büyük ölçekli yerçekimi sabitine bağlıdır. Bu çalışmada, farklı zamanlarda iki operatörün kullanılması ve sırayla çalışmalarını kapsayan yeni algoritma önerilmiştir ve Sıralı Değiştirilmiş Yerçekimi Arama Algoritması (SMGSA) olarak adlandırılmıştır. SMGSA 10 temel ve 6 kompozit kıyaslama fonksiyonuna uygulanmaktadır. Her fonksiyon 30 kez çalıştırılır ve en iyi, ortalama ve medyan değerler elde edilmektedir. Elde edilen sonuçlar sezgisel optimizasyon algoritmaları arasında Genetik Algoritma (GA), Parçacık Sürüşü Optimizasyonu (PSO) ve GSA ile karşılaştırılmıştır. GSA ile operatör arasında her fonksiyon yakınsama hızı için standart sapma ve grafik karşılaştırmalar bulunmuştur. Bunun yanı sıra, Wilcoxon sıralama testi kullanılarak, verilerin ortalamalarının iki bağımlı GSA grubu ve yeni operatörler olarak karşılaştırılması gerçekleştirilmiştir. Ayrıca bu çalışmada, mühendislik uygulamalarından görüntü iyileştirme

teknikleri arasında yer alan dönüşüm fonksiyonuna SMGSA uygulanmıştır. Bu yöntemin başarısı, kullanılan dönüştürme fonksiyonunun parametreleri optimize edilerek artırılmıştır. Hem görsel hem de bilgi kalitesi açısından etkili bir gelişme sağlanmıştır.

Anahtar Kelimeler: Yerçekimi Arama Algoritması, Optimizasyon, Görüntü İyileştirme

I. INTRODUCTION

“Optimum” is a Greek word and means the final result based on the available possibilities. Derived from this word, optimization similarly means the method for finding the most appropriate solution under decision variables and restrictions in order to solve different problems [1]. Optimization methods are commonly divided into two groups. The first of them are the deterministic techniques able to generate the appropriate solution, and the second are heuristic techniques generating the optimal solution. Heuristic algorithms among the optimization techniques are algorithms which are inspired by behavior in natural life in order to realize any purpose or to reach the target and have a very simple structure with regards to intelligibility [2]. This study deals with the improvement of the GSA, which is a heuristic technique and based on Newton’s law of gravity and movement. According to the Law of Gravity, every agent attracts other agents and the gravitational force between both agents is directly proportional to the direct multiplication of the masses of both agents and inversely proportional to the distance between each other. The update of the Law of Movement in this algorithm is the valid speed of any agent equal to the sum of the deviation of the speed and its previous speed value [3].

Many modification studies are performed by making changes and improvements via the variables and parameters within the GSA optimization algorithm. Studies on the gravitational constant among these modification studies hold an important place. The Pareto optimal method, providing rapid selective classification and exclusion effect in order to calculate the G_0 start value of the gravitational constant in the most appropriate and adaptive manner at the multipurpose gravitational search algorithm containing the non-dominant classification concept [4]. In another study is a new gravitational constant function designed, which is a sort of a piecewise function. A piecewise function divided into three pieces is used in order to control the decrease ratio of the gravitational constant. The divided three pieces are called rough search status, medium stage search and fine search status respectively and approach to and obtainment of the optimal value is performed [5]. Cloudy adaptive dynamic gravitational constant design works are performed by using the cloudy IF/THEN rules. The position and speed updates within the concepts are the same as the classical GSA. But the gravitational constant is adjusted dynamically the greater the cycle gets by using the IF/THEN rules, see Refs. 6 and 7 for examples [6, 7]. Also, the standard GSA consists of gravitational constant positive figures. In another developed algorithm is also the grey level of the image is added to the calculation of the gravitational constant and a gravitational constant resulting in integers is obtained. Also, image segmentation is used at the multiple level thresholding work [8]. Cloudy logic works are performed on the alpha parameter, which holds an important position at the determination of the size of the gravitational constant. Sombra et al. have worked with the cloudy logic on the variation of the alpha parameter within the iteration. Saeidi-Khabisi et al. have obtained an exit, providing the alpha and previous alpha values while the population diversity and progress constituted the entrance of the cloudy system [9-10]. Adaptive gravitational constant and global best agent normal mutation are suggested at the other new operator work used at the segmentation of multi layered images in order to derive the agents from the local minimum and to improve the calculation accuracy [11]. In two aspects modified GSA is used at the hydro energy turbine management of hydro energy generation units. As the first phase is the gravitational constant decrease function, serving to balance the global search and local exploitation, replaced with the hyperbolic function. And secondly agent mutation is applied in order to strengthen the jump from the local minimum feature of the GSA as it was the case in the first study [12]. In one of the recent studies was proposed a new variant of GSA, namely stability constrained adaptive alpha for GSA. Each agent's evolutionary state is estimated, which is then combined with the variation of the agent's position and fitness feedback to adaptively adjust the value of α [13]. Another study, new operator called “escape velocity” has been

proposed which is inspired by the real nature of GSA. It has been suggested that adding the escape velocity negatively will enable the agents that remain far away or outside of group behavior to be included in the group or to be increased in velocity [14]. Finally, Kang and his friends proposed the hybrid gravitational search algorithm to increase the utilization of particle information and to facilitate thorough search inside the video frame before convergence. This study elegantly combines GSA's gravitational update component with the cognitive and social components of PSO using a novel weight function [15].

Image enhancement aims to reduce or remove deterioration in an image or to improve the image for a specific purpose using human observation or computer analysis methods [16]. Histogram Equalization (HE), a primary method used to adjust contrast and brightness, performs appropriate changes on pixel values of the input image and provides equalization against each pixel value of the output image [17]. Implementation of this method provides easy and fast results. Over the next time, many improved versions of HE have been proposed [18-20]. Most researchers preferred a sigmoid function to improve the contrast and brightness of an image. Tanaka et al. used a generalized sigmoid, Kannan et al. recommended a modified sigmoid function, Verma et al. recommended another modified sigmoid function by using Particle Swarm Optimization (PSO) algorithm [21-23]. Image improvement was performed by applying GA on a transformation function called the Local Transformation Function (LTF). An objective evaluation criterion was maintained by multiplying the Sobel value, entropy value, and number of edges of the image [24]. Later, LTF was applied on the PSO by Gorai and Ghosh in 2009, on Zhao GSA in 2011, on Cuckoo Search Algorithm by Agrawal and Panda in 2012, on Differential improvement algorithm by Sarangi et al. in 2014, and on Grey-Wolf Optimizer algorithm by Murali and Jayabarathi in 2016 [25-29].

In recent years, there has been an enhancement in gray level images using heuristic optimization algorithms. In one of these studies, Nickfarjam and Komleh proposed a multi-resolution method for gray-level image enhancement using Particle Swarm Optimization. The method has been employed the ability of image pyramid to determine informative parts of an image for visual perception [30]. Dhal et al's work includes an up-to-date review over the application of nature-inspired optimization algorithms in image enhancement domain. The key issues which are involved in the formulation of optimization algorithms-based image enhancement models were also discussed here [31]. A novel image quality enhancement framework was proposed through a collective inspiration of the exponential, differential and linear operational behavior of pixel intensities by Singh et al's. Here, a new mask framing strategy was presented for harvesting the benefits of optimally ordered fractional differential unsharp masking [32]. As the last study, a novel krill herd based optimized contrast and sharp edge enhancement framework is introduced for medical images by Kandhway et al's. Plateau limit and fitness function were proposed in this paper to achieve the best-enhanced image. A new plateau limit was applied to clip the histogram using minimum, maximum, mean, and median of the histogram with a tunable parameter [33].

After examining the GSA algorithm, it has been determined that the GSA algorithm has two disadvantages such as being stuck to the local minimum and not making sensitive calls.. In this study, in the first operator, changes were made in the velocity and consequently positions of the agents by creating chaotic shake on the gravitational constant in cases of being stuck in a local minimum and searching away from the appropriate global value. The aim of the last operator is to ensure that the total force and consequently velocity are low by activating the agents with the worst mass when finding the total force of an agent with the best result value in the next iteration. As a result of this study, it will be provided to be preferred in engineering applications such as image enhancement with flexible and practical optimization algorithm.

In this study, first the description of the gravitational search algorithm is made. In the same section is explained the chaotic shake operator which reduction of sticking to local minimum or worst sector problem. And then is introduced the best agent operator which has precise search capability. Sequentially doing works logic of chaotic shake and the best agent operators has been included in SMGSA which was proposed in third section. The aim is not to fall to the local minimum in the first

stages of the call, but to perform precision calls in the last stages. The fourth section includes the results of the performed applications and the suggested algorithm and the standard GSA are presented comparatively. Also, at the end of this section, the proposed algorithm is applied to the image enhancement problem. In the final section are answers searched for questions like how our study influences the search results, what can be said with regards to the most appropriate values of the parameters.

II. GRAVITATIONAL SEARCH ALGORITHM

In this section, an optimization algorithm GSA based on the law of gravity is introduced. All these objects attract each other by gravitational force, and this force causes the movement of all objects towards the objects with bigger masses [34]. Now consider a system with N -agent(mass). The location of the i .th agent is defined by the following expression;

$$X_i = (x_i^1, \dots, x_i^d, \dots, x_i^n) \quad i = 1, 2, \dots, N \quad (1)$$

Eq. (1) in the formula is defined as the dimension of the problem and X_i is defined as the position of i .th agent in the d .th dimension. The force movement from j mass on i mass in a given t time is defined as follows;

$$F_{ij}^d(t) = G(t) \frac{M_{pi}(t) \cdot M_{aj}(t)}{R_{ij}(t) + \varepsilon} (x_j^d(t) - x_i^d(t)) \quad (2)$$

Where M_{aj} is the active gravitational mass related to agent j , M_{pi} is the passive gravitational mass related to agent i , $G(t)$ is gravitational constant at time t , ε is a small constant, and $R_{ij}(t)$ is the Euclidian distance between two agent i and j . The total force on the i agent within d dimension is expressed as randomly aggravated d .th components in order to give the stochastic characteristic to algorithm.

$$F_i^d(t) = \sum_{j=1, j \neq i}^N rand_j F_{ij}^d(t) \quad (3)$$

In the Eq. (3), $rand_j$ is a random number in the interval [0,1]. The acceleration of i . agent by using above equation and the laws of motion.

$$a_i^d(t) = \frac{F_i^d(t)}{M_{ii}(t)} \quad (4)$$

M_{ii} expression in the equation represents the inertial mass of the agent. Position and velocity of the agent can be calculated as follows.

$$v_i^d(t+1) = rand_i \cdot v_i^d(t) + a_i^d(t) \quad (5)$$

$$x_i^d(t+1) = x_i^d(t) + v_i^d(t+1) \quad (6)$$

Again, the $rand_i$ in the first equation above is a random value in the range of [0,1] and it is used to give a random characteristic to the study. $G(t)$, of which gravitation is constant, will be reduced to control the search accuracy, and so, it has been launched with a constant value initially. In other words, the initial value of $G(t)$ is G_0 and it is a function of time.

$$G(t) = G_0 * \exp\left(-\alpha \cdot \frac{iter}{max_iter}\right) \quad (7)$$

Assuming that gravitational and inertial masses are equal, it can calculate the values of masses by using fitness map. Gravitational and inertial masses can be updated by the following equation.

$$M_{ai} = M_{pi} = M_{ii} = M_i \quad i = 1, 2, \dots, N \quad (8)$$

$$m_i(t) = \frac{fit_i(t) - worst(t)}{best(t) - worst(t)} \quad (9)$$

$$M_i(t) = \frac{m_i(t)}{\sum_{j=1}^N m_j(t)} \quad (10)$$

in the Eq. (9), $fit_i(t)$ represents the fitness value of i agent in t time and, $worst(t)$ and $best(t)$ are defined as following:

$$best(t) = \min_{j \in \{1, \dots, N\}} fit_j(t) \quad (11)$$

$$worst(t) = \max_{j \in \{1, \dots, N\}} fit_j(t) \quad (12)$$

GSA algorithm steps are given below [34].

1. Defining the search space
2. Random start
3. Evaluate the fitness values of agents
4. Updating the values of $G(t)$, $best(t)$, $worst(t)$ and $M_i(t)$ for $i = 1, 2, \dots, N$ again.
5. The calculation of the total force in different directions
6. Acceleration and velocity calculations
7. Updating the position of agents
8. Repeating the steps from 3 to 7 until reaching the criteria given
9. End.

A. CHAOTIC SHAKE GRAVITATIONAL SEARCH ALGORITHM (CSGSA)

The gravitational constant $G(t)$ in the GSA is an important variable, used at changing the places of the agents within the search space, and determining the speeds of the agents. It is included in the formula regarding the force influencing the agent in Eq. (2), but its influence reaches up to the agent speeds, which are important for the search. At the initial iterations of the algorithm has the gravity high values and results in high strengths of the gravitational forces. And this results in the rapid movement agents during the initial iterations. The rapid movement of the agents is a desired situation for the first phases of the search.

According to the decreasing function in Eq. (7) will the $G(t)$ value progressively decrease, and the speed of the agents will decelerate and a clustering around the agents will incur with slow movements due to the gravitational force of the heavy agents. This is called the “accurate search status” and it is provided that this happens during the last iterations. If a tripping into the local status should happen after a definite iteration as of the start of the search, the agents can’t leave this region while reaching the last iterations and the search will result in bad values. It is stated in the majority of the studies performed for GSA during previous years that tripping into the local minimum during early iterations and later the not ability to leave the local minimum point due to the deceleration of the speeds of the agents when approaching the last iterations is one of the disadvantages of this algorithm [35-38].

Also, how to determine the tripping status of the GSA into the local minimum during the search process is as important as the solution of the problem. For this can particularly the best value determined for each iteration be compared with the previous one and inferences can be made with regards to the search process. In particular, when the best result value doesn’t change during start and medium phases of the

search while the iteration number increases, it is resulted that it is tripped into the local lowest value or the search is being performed in the bad sectors.

In order to approach the local minimum and release the tripped agents there and to direct them to new search sectors, it is first necessary to determine the situation of tripping into the local minimum. According to chaotic shake operator, when the global best value doesn't change, then the "Number of unchanging" value increase by one and when the situation of not changing should occur also in the subsequent iterations, then the "Number of unchanging" value will continue to increase. In this case it can be seen by looking at the "Number of unchanging" value that no changes have occurred at how many iterations and how many iterations are tripped into the local minimum [39]. After having determined the problem, the speeds and positions of the agents are changed by generating a small shake on the gravitational constant in order to avoid the local minimum and convert the search algorithm dynamic [40].

Table 1. Chaotic functions used at the chaotic shake operator.

N	Name	Chaotic function	Range
1	Circle map	$X_{i+1} = \text{mod} \left(X_i + b - \left(\frac{a}{2\pi} \right) \sin(2\pi X_i), 1 \right),$ $a = 0.5 \text{ and } b = 0.2$	(0,1)
2	Logistic map	$X_{i+1} = aX_i(1 - X_i), \quad a = 4$	(0,1)
3	Singer map	$X_{i+1} = \mu(7.86X_i - 23.31X_i^2 + 28.75X_i^3 - 13.302875X_i^4),$ $\mu = 1.07$	(0,1)
4	Sinüzoidal map	$X_{i+1} = aX_i^2 \sin(\pi X_i), \quad a = 2.3$	(0,1)

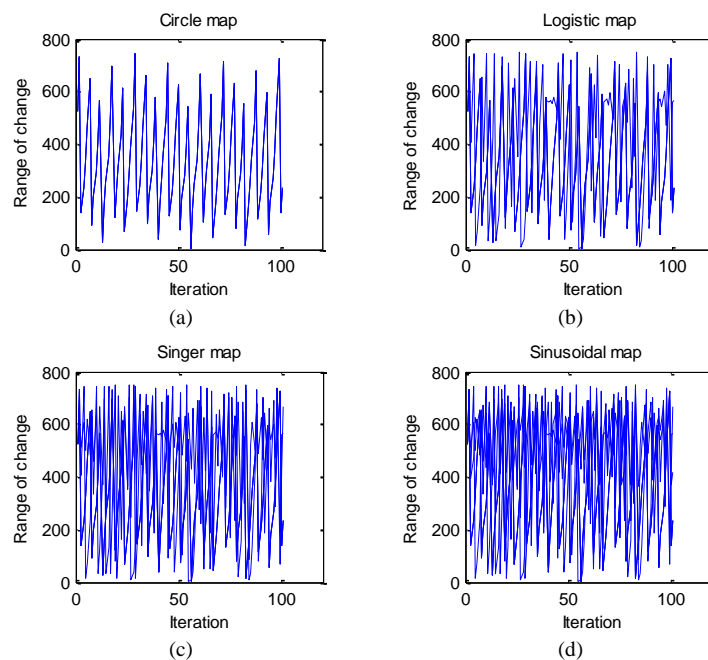


Figure 1. Views of the chaotic maps.

A chaotic shake is generated when the number of the cycle is less than 50%, meaning when it is at the first or medium phases of the search and the best result value didn't change by the "Threshold" figure. Thus, it is provided that the search is shifted to other sectors. When it is except these conditions, the status "normal search is being performed" is continued. By generating a chaotic shake are the necessary agent speeds ensured in order to relief from this situation in case of tripping into the local minimum and the realization of a bad search [41].

Non chaotic linear determinism is defined as complex behavior [42]. The first definition of a chaotic process is performed by Lorenz in 1963 and used at non-linear differential equation systems known as Lorenz Attractor in order to model sun patterns [39]. It is used in the literature at some engineering applications like signal processing, chaos control, safety communication [44-46].

$$G(t) = Shake + G_0 \cdot \exp\left(-\alpha \cdot \frac{iter}{max_iter}\right) \quad (13)$$

In the iteration, where chaotic shake will be applied when the most appropriate value doesn't change, is Eq. (13) applied instead of the gravitational constant expression in Eq. (7).

The chaotic maps, named in Eq. (13) above as "Shake" and used at the study, are presented in Table 1. The Circle, Logistic, Singer and Sinusoidal functions, widespread used in the literature, are preferred [47-50]. The random feature providing components are not included into the chaotic maps used in Table 1.

Fig. 1. indicates the output graphics of the determinism systems able to ensure chaotic behaviors. The chaotic behaviors of the equations indicated in Fig. 1 are rather significant. Different behaviors can be selected while the cluster start points of the chaotic maps are 0.7. Any figure between 0 and 1 can be selected for the starting point.

B. THE BEST AGENT GRAVITATIONAL SEARCH ALGORITHM (BAGSA)

There is a gravitational force between the masses in the GSA. The mass of the agent with the best result value in each cycle has the greatest value as indicated in Eq. (9). The gravitational force is proportional to the mass of the objects and inversely proportional to the square of the distance between them. Also, the direction of the gravitational force is towards the large object. So, objects with large mass move slowly.

The total force on the agent i in dimension d is calculated in two ways in Eq. (2). In the first, it is expressed as the sum of the forces of all agents that affect the agent i . Second, it is desirable to improve the performance of the GSA by reducing the number of agents in each iteration and controlling exploration and exploitation. $Kbest$ is a function of time, initially all agents will apply force to the corresponding agent and $Kbest$ will decrease linearly in each cycle as time passes. In the last iteration, agents as much as $final_per$ that will be specified in the program will affect the relevant agent. The reduction rate in $kbest$ has also been shown mathematically in the following Eq. (14) [51].

$$Kbest = final_per + \left(1 - \frac{iteration}{max_it}\right) * (100 - final_per) \quad (14)$$

$$F_i^d(t) = \sum_{j \in Kbest, j \neq i}^N rand_j F_{ij}^d(t) \quad (15)$$

According to Eq. (15), the agents affecting it are selected among the agents with the best masses. This also means that an agent with too large mass has big acceleration, speed and it substantially changes position as others. However, it is expected that it will move very slowly because of its greatest value and its mass. In order to remove the drawback determined above, the $Kworst$ application has been aimed at, which is a special application complete opposite to $Kbest$ approach, when finding the total force of the agent with the vest result value in the next iteration. $Kworst$ application is regulated in Eq. (16), and the affecting total force calculation of the best agent is regulated in Eq. (17).

$$Kworst = final_per + \left(1 - \frac{iteration}{max_it}\right) * (100 - final_per) \quad (16)$$

$$F_i^d(t) = \sum_{J \in K_{worst}, j \neq i}^N rand_j F_{ij}^d(t) \quad (17)$$

Total force, consequently the speed will be low by commissioning the agents with the worst mass affecting this agent in *Kworst* approach. It will increase convergence feature to best result value through position change at very small rates.

Firstly, the agent index with the smallest value among the fitness values in the previous cycle is given to the variable called “*En*”. Afterwards, those with the smallest masses are allowed to be processed by arraying oppositely to others when the turn comes to the best agent with *En* index. When the agents with small masses are added while calculating the total force of the best agent, *Kbest* approach is continued in other agents, and those with big masses were enabled to participate [51].

III. SEQUENTIALLY MODIFIED GRAVITATIONAL SEARCH ALGORITHM (SMGSA)

SMGSA is based on the sequential doing work logic of chaotic shake and the best agent operators. The aim is not to fall to the local minimum in the first stages of the call, but to perform precision calls in the last stages.

1. Defining the search space
2. Random start
3. Iter. <= %50 Max_Iter.,
Chaotic Shake Operator

4. Evaluating the *fitness*
5. *G(t)* with Chaotic Shake
Make chaotic shake if best value does not change
6. Updating of *best(t)*, *worst(t)* and *Mi(t)*
7. The calculation of the total force
8. Acceleration and velocity calculations
9. Updating the position of agents

- Iter. > %50 Max_Iter.
The Best Operator

4. Evaluating the *fitness*
5. Find The Best Agent
6. Updating of *G(t)* *best(t)*, *worst(t)* and *Mi(t)*
7. The calculation of the total force
Apply the best agent *Kworst* technique
8. Acceleration and velocity calculations
9. Updating the position of agents

10. Repeating the steps from 3 to 9 until reaching the criteria given
11. End.

Primarily, it is inquired at the beginning of each cycle whether the best result at the previous iteration changed or not. Thus, an idea is obtained on whether it has tripped into the local minimum or not. The update of *G(t)* is separated from the updates of the best and worst agent and performed during the previous phase. Chaotic shake is generated when the “Number of unchanging” value is equal to and higher than the threshold value and *G(t)* is updated.

In the second stage of the search, the agent with the best value is found among the fitness values. In total force calculation, when the turn comes to this agent, those with small masses are allowed to be processed by arraying completely opposite to others.

IV. EXPERIMENTAL RESULTS

A. EVALUATION RESULTS OF SMGSA'S BASIC TEST FUNCTIONS

Benchmark functions are used for the performance tests of the SMGSA. As to be seen in Table 2, n indicates the dimension figure of the function and the search space $S \subseteq \mathbb{R}^n$ is defined as the sub-cluster of the real figures' cluster. The ratio in the parenthesis indicates the limits of this function within the search space. The first three functions given in Table 2 are unimodal functions and are preferred in order to provide rather the convergence speed of the algorithm than the result value of the optimization. Three subsequent functions are multimodal functions and the dimension size is high. There are many local minimum points within these functions. Therefore, the aim at running these functions is to see how far they approach the global best value and whether they trip into the local minimum or not. Last four functions in Table 2 belong to the multimodal functions group and the dimension number and limit range are low compared with the second group. The number of the local minimums is low. Therefore is the number of the iterations kept low when working in this function group and looked at the process duration and the closeness criterion to the best value for each operation [52].

Table 2. Basic test functions.

Nr	Test Function	Dimension
1	$F_1(X) = \sum_{i=1}^n X_i^2$	$[-100,100]^n$
2	$F_3(X) = \sum_{i=1}^n (\sum_{j=1}^i X_j)^2$	$[-100,100]^n$
3	$F_6(X) = \sum_{i=1}^n ([X_i + 0.5])^2$	$[-100,100]^n$
4	$F_8(X) = \sum_{i=1}^n -X_i \sin(\sqrt{ X_i })$	$[-500,500]^n$
5	$F_{10}(X) = -20 \exp\left(-0.2 \sqrt{\frac{1}{n} \sum_{i=1}^n X_i^2}\right) - \exp\left(\frac{1}{n} \sum_{i=1}^n \cos(2\pi X_i)\right) + 20 + e$	$[-32,32]^n$
6	$F_{12}(X) = \frac{\pi}{n} \left\{ 10 \sin(\pi y_1) + \sum_{i=1}^{n-1} (y_i - 1)^2 [1 + 10 \sin^2(\pi y_{i+1})] + (y_n - 1)^2 \right\} + \sum_{i=1}^n u(X_i, 10, 100, 4)$ $y_i = 1 + \frac{X_i + 1}{4}$ $u(X_i, a, k, m) = \begin{cases} k(X_i - a)^m X_i > a \\ 0 & -a < X_i < a \\ k(-X_i - a)^m X_i < -a \end{cases}$	$[-50,50]^n$
7	$F_{14}(X) = \left(\frac{1}{500} + \sum_{j=1}^{n25} \frac{1}{\sum_{i=1}^2 (X_i - a_{ij})^6}\right)^{-1}$	$[-65.53, 65.53]^2$
8	$F_{15}(X) = \sum_{i=1}^{11} \left[a_i - \frac{X_1(b_i^2 + b_i(X_2))}{b_i^2 + b_i(X_3 + X_4)} \right]^2$	$[-5,5]^4$
9	$F_{19}(X) = -\sum_{i=1}^4 c_i \exp\left(-\sum_{j=1}^3 a_{ij}(X_j - p_{ij})^2\right)$	$[0,1]^3$
10	$F_{23}(X) = -\sum_{i=1}^{10} [(X - a_i)(X - a_i)^T + c_i]^{-1}$	$[0,10]^4$

The variables within the SMGSA are taken as $G_0=100$, $\alpha=20$, $N=30$. The iteration for first six functions in Table 2 is 1000, and the iteration for last four functions is 500 and the dimension is variable for each function. These indicated values are selected as the most appropriate values and not changed during the experiment process. The GSA, BAGSA, CSGSA and SMGSA are operated each 30 times for every function worked on. Each problem was solved 30 times independently and with different random initial seeds to determine the reliability of the optimization algorithm. Calculations were performed for a certain number of iterations and then stopped. The best value, average of the results and median values are obtained as a result of each 30 operations.

The comparison method is the most important method for testing the performances of the obtained operators. The first is GA, among the heuristic algorithms is a search and optimization method developed basically based on the natural evolution process. There are different versions developed during the subsequent years of the algorithm invented by John Holland. The GA version among these is added as the comparison algorithm [53]. PSO is developed in 1995 by Dr. Eberhart and Dr. Kennedy and is based on the behavior of bird swarms [54]. Finally is the standard GSA, BAGSA and CSGSA taken as a reference study [34, 55].

As a second approach is the Wilcoxon signed-rank test used at the evaluation of the obtained results. The aim at this test was the comparison of the numeric data obtained from the standard GSA and the developed operators. Wilcoxon signed-rank test is a strong test and that it takes into consideration the amount of the difference without regard to the sign (whether being negative or positive) between the differences. The sum of the orders of the positive and negative differences need to be zero for the correctness of the zero hypothesis [56, 57]. While the zero hypothesis is accepted when it is greater, it indicates in the contrary case that there is a great difference and thus that the developed algorithm is strong [58].

At the last evaluation is the average of the process durations taken for the standard deviation and single iteration after each 30 operations. The standard deviation is the square root of minus one of the divisions of the sum of the differences of the figures in a figure array from the arithmetic average of the figures. Standard deviation indicates how the data is distributed in itself. That the standard deviation is low, indicates that the values are close to each other, and high, indicates that the values are far from each other. The process duration is calculated for a single cycle and is important with regards to providing an idea about the speed of the algorithm.

Table 3. Minimized results of the CSGSA at unimodal test functions.

F.		GA [52]	PSO [52]	GSA [27]	BAGSA	CSGSA	SMGSA
f_1	Best	9.6732	$1.1 \cdot 10^{-4}$	$9.41 \cdot 10^{-19}$	$2.88 \cdot 10^{-20}$	$3.48 \cdot 10^{-21}$	$6.179 \cdot 10^{-23}$
	Median	21.3478	$1.4 \cdot 10^{-3}$	$2.11 \cdot 10^{-18}$	$4.13 \cdot 10^{-20}$	$9.41 \cdot 10^{-21}$	$8.810 \cdot 10^{-23}$
	Mean	23.1591	$2.3 \cdot 10^{-3}$	$2.21 \cdot 10^{-18}$	$8.10 \cdot 10^{-17}$	$8.10 \cdot 10^{-17}$	$8.676 \cdot 10^{-23}$
f_2	Best	395.78	139.77	98.35	2.155	$3.020 \cdot 10^{-7}$	$2.056 \cdot 10^{-7}$
	Median	569.10	226.89	222.21	2.438	$6.654 \cdot 10^{-7}$	$2.525 \cdot 10^{-7}$
	Mean	561.68	411.45	238.12	8.795	2.772	$3.64 \cdot 10^{-7}$
f_3	Best	4.1165	$6.12 \cdot 10^{-3}$	$9.45 \cdot 10^{-17}$	0	0	0
	Median	24.5645	$6.68 \cdot 10^{-3}$	$2.11 \cdot 10^{-16}$	0	0	0
	Mean	24.0321	0.0009	$2.11 \cdot 10^{-16}$	0	0	0
f_4	Best	$-1.2 \cdot 10^4$	$-1.06 \cdot 10^4$	$-3.67 \cdot 10^3$	$-7.05 \cdot 10^3$	$-7.13 \cdot 10^3$	$-9.054 \cdot 10^3$
	Median	$-1.2 \cdot 10^4$	$-2.79 \cdot 10^3$	$-2.91 \cdot 10^3$	$-6.15 \cdot 10^3$	$-6.59 \cdot 10^3$	$-6.991 \cdot 10^3$
	Mean	$-1.2 \cdot 10^4$	$-9.98 \cdot 10^3$	$-2.91 \cdot 10^3$	$-5.27 \cdot 10^3$	$-6.66 \cdot 10^3$	$-6.772 \cdot 10^3$
f_5	Best	1.3425	0.0034	$2.87 \cdot 10^{-9}$	$2.27 \cdot 10^{-9}$	$2.18 \cdot 10^{-9}$	$8.04 \cdot 10^{-12}$
	Median	2.1342	0.0085	$3.87 \cdot 10^{-9}$	$3.49 \cdot 10^{-9}$	$2.50 \cdot 10^{-9}$	$2.24 \cdot 10^{-12}$
	Mean	2.1458	0.0089	$3.44 \cdot 10^{-9}$	$3.92 \cdot 10^{-9}$	$3.94 \cdot 10^{-9}$	$1.97 \cdot 10^{-9}$
f_6	Best	0.0139	0.0006	$6.65 \cdot 10^{-20}$	$3.14 \cdot 10^{-20}$	$3.59 \cdot 10^{-20}$	$3.80 \cdot 10^{-24}$
	Median	0.0378	0.2311	$2.54 \cdot 10^{-19}$	$1.23 \cdot 10^{-19}$	$5.89 \cdot 10^{-20}$	$4.92 \cdot 10^{-24}$
	Mean	0.0562	0.2345	0.0498	$4.21 \cdot 10^{-19}$	$7.03 \cdot 10^{-20}$	$5.03 \cdot 10^{-24}$
f_7	Best	0.9980	0.9980	0.9980	0.9980	0.9980	0.9980
	Median	0.9980	0.9980	3.30	0.9980	0.9980	0.9980
	Mean	0.9980	0.9980	4.72	1.8293	1.6593	1.1965
f_8	Best	0.0011	$3.07 \cdot 10^{-4}$	0.0016	$8.22 \cdot 10^{-4}$	$3.84 \cdot 10^{-4}$	$3.07 \cdot 10^{-4}$
	Median	0.0017	$7.02 \cdot 10^{-4}$	0.0022	0.00118	0.00103	$5.08 \cdot 10^{-4}$
	Mean	0.0040	0.0028	0.0018	0.00126	0.00107	$8.97 \cdot 10^{-4}$
f_9	Best	-3.8628	-3.8628	-3.8628	-3.8628	-3.8628	-3.8628
	Median	-3.8628	-3.8628	-3.8628	-3.8628	-3.8628	-3.8628
	Mean	-3.8627	-3.8628	-3.8628	-3.8628	-3.8628	-3.8628
f_{10}	Best	-	-10.5364	-10.5364	-10.5364	-10.5364	-10.5364
	Median	-4.5054	-10.5364	-10.5364	-10.5364	-10.5364	-10.5364
	Mean	-6.2541	-9.7634	-10.5364	-10.5364	-10.5364	-10.5364

As to be seen in Table 3 are the comparison charts for each unimodal, high dimensional test functions with SMGSA and the frequent used method in the literature, GA, PSO and standard GSA algorithms are given. When the table is examined, it is determined that the improvement is significant at the functions F1, F2 and F3. For multimode and high dimensional functions, it is to be seen that the results

and the performances are attracting the attention at the test functions F5 and F6. For multimodal and low dimensional test function SMGSA has shown a good performance and positive results are realized at very low rates due to the features of the functions. The great variation between both algorithms is at the functions F7.

In Fig. 2. F1 and F2 are the graphics of the best results for test functions as a result of a single operation indicated. It is seen that the convergence speeds are higher at function F1 and F2 compared with the standard GSA and that the result values are lower. The best averages of the functions F4 and F5 the more the iteration progresses which is seen on both graphics that it is better than the standard GSA, BAGSA and CSGSA with regards to achieving the global value and the approach speed to the global value and the accurate search feature. In Fig. 5. F8 and F10 are the improvement, even if very low, in favor of the SMGSA.

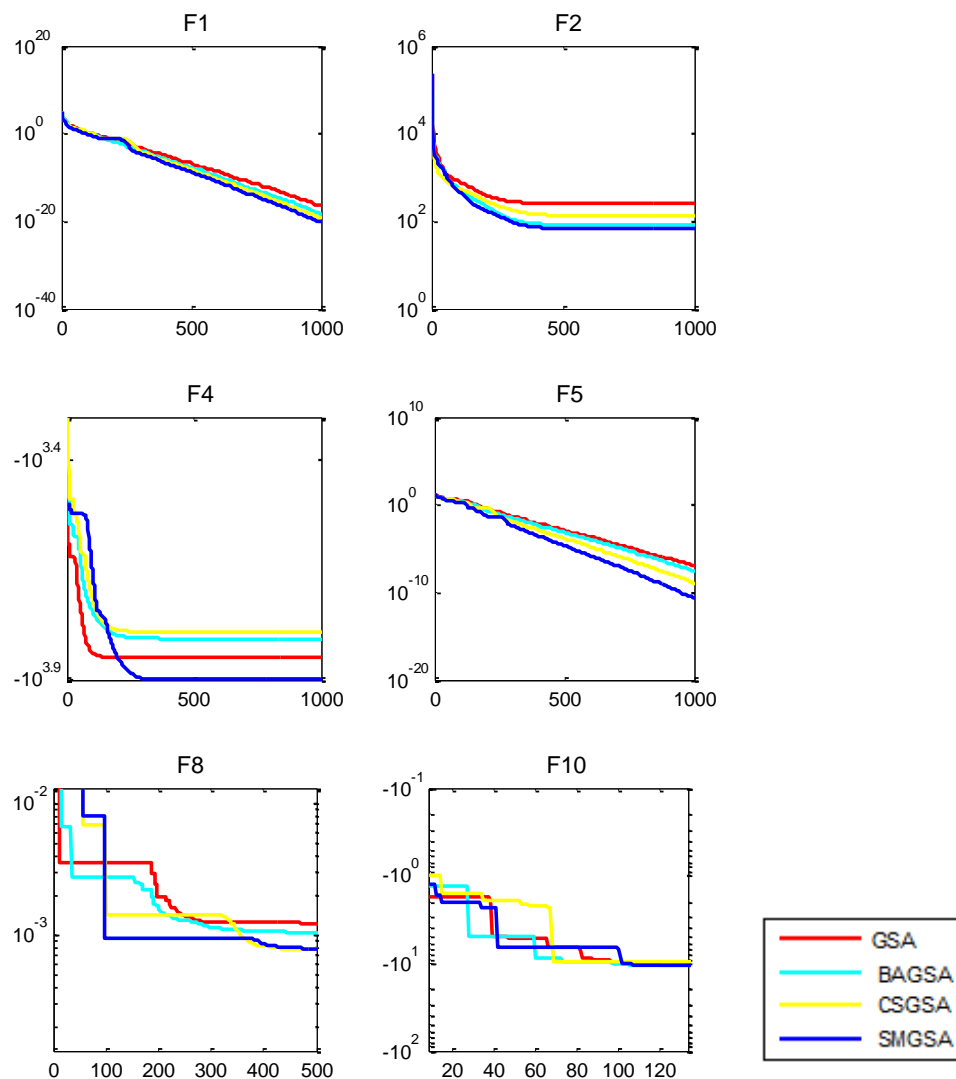


Figure 2. Comparison of the convergence feature of the GSA, BAGSA, CSGSA and SMGSA at basic functions. F1 and F2: Unimodal test functions, F4 and F5: Multimodal test functions, F8 and F10: Multimodal test functions with low dimensions.

Table 4. Wilcoxon signed-rank test result for SMGSA F1

Parameters	GSA	SMGSA
Numerosity	30	30
Sum of Ranks (W)	1365.0	465.0
Mean rak.	45.5	15.5
Test variable (U)	0.0	900.0
Sample size is large enough to normal dist. apron.		
Mean	450.0	
Z	6.6456	6.6456
p-value (1-tailed)	0.00000	
p-value (2-tailed)	0.00000	

As to be seen in Table 4 is Wilcoxon signed-rank test applied to function F1. The most important issue to be paid attention here is that the value in the last line among the p values in the table has to be taken into consideration since a dual comparison is being performed. The zero hypothesis is rejected since the obtained z value is higher than 3.5 and has the p value of 0.0000. This means that there are significant differences for this function between GSA and SMGSA and the developed operator is strong.

In Table 5 are not all parameters of the array test indicated, but only the p value, determining the hypothesis result. The functions F1-F7 approve the zero hypothesis is rejected, it is understood at the others from that the p threshold value is lower than 0.05 that there are great differences between the GSA and the SMGSA.

The zero hypothesis is realized at the F8-F10. Prior to setting over to the reason for this, it will be seen in Table 3 when attentively examined that the GSA and SMGSA results for these functions are all same or very close to each other. Therefore, this resulted in that the z value was very low and the p value as 2.00000. The importance level $p=0.05$ hypothesis greater than zero is approved, there are no differences between both algorithms.

Table 5. Standard deviation, Time and Wilcoxon Signed-rank comparison between GSA and SMGSA

Method		f_1	f_2	f_3	f_4	f_5	f_6	f_7	f_8	f_9	f_{10}
St.Dev.	GSA	1.1.10-15	122.9	0.305	7.68.10+2	1.08.10-9	0.2280	7.1.10-15	1.2.10-4	1.3.10-5	0.875
	SMGSA	2.3.10-17	117.0	0.182	7.07.10+2	1.08.10-11	0.0316	2.2.10-16	1.9.10-4	2.1.10-10	0.259
Time	GSA	0.0040	0.0052	0.0042	0.0040	0.00411	0.0051	0.0039	0.0016	0.0017	0.0015
	SMGSA	0.0041	0.0054	0.0044	0.0041	0.00431	0.0053	0.0040	0.0022	0.0020	0.0021
Wil. Sig-r		0.00000	0.00000	0.00312	0.00016	0.00037	0.00002	0.00065	0.25188	2.00000	2.00000

The standard deviation is lower for all functions at the SMGSA. In Table 5 Time line indicate the comparison of the process duration of both applications. The process duration resulted higher compared with GSA under equal iterations. The addition of chaotic functions and the generation of shakes have increased the process duration.

The function F8 in Fig. 3. (a) is operated each once and the graphics for the decrease ratios of the gravitational constant according to the iteration are given. The function F8 in Fig. 3. (b) reflected positively on the result values since a very intensive chaotic shake is generated between iterations 50 and 300.

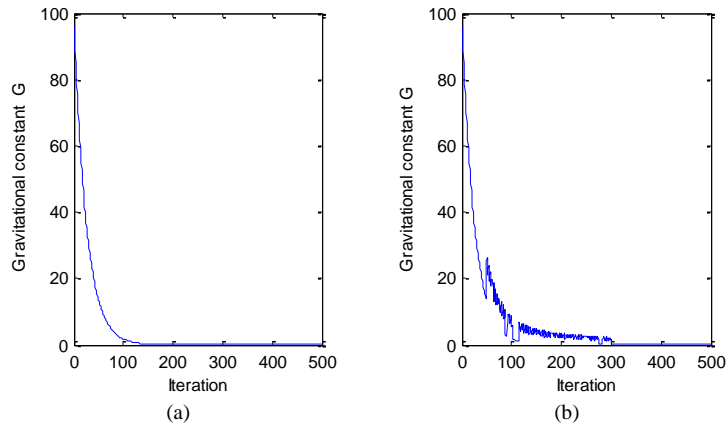


Figure 3. Comparison of the convergence feature of the GSA and SMGSA at F8 test functions, (a) Change curve of the gravitational constant at GSA for F8, (b) Change curve of the gravitational constant at SMGSA for F8.

The function F5 is selected and iterations is kept at a low value of 300 in order to see the chaotic shakes better and to examine them. Shake is generated for the same range between 50 and 250 for each chaotic function. Table 6 indicates the output curves of the chaotic functions preferred at the application work and the operator under the same conditions. It is seen that the Singer and Logistic in Table 6 are more variable with regards to changing the $G(t)$ value. This feature resulted in that the contributions of the two chaotic maps were better. The results of the Singer map in Table 6 are attracting the attention.

Table 6. Performance results of chaotic functions.

F5 N=30 Iteration=300 $\alpha=20$ $G_0=100$ 50-250 Chaotic Shake	Circle	Logistic	Singer	Sinusoidal
Best	$4.71 \cdot 10^{-9}$	$3.43 \cdot 10^{-9}$	$3.20 \cdot 10^{-9}$	$3.65 \cdot 10^{-9}$
Median	$4.79 \cdot 10^{-9}$	$4.01 \cdot 10^{-9}$	$4.03 \cdot 10^{-9}$	$4.35 \cdot 10^{-9}$
Mean	$5.07 \cdot 10^{-9}$	$4.35 \cdot 10^{-9}$	$4.15 \cdot 10^{-9}$	$4.24 \cdot 10^{-9}$
S. Deviation	$5.49 \cdot 10^{-10}$	$6.49 \cdot 10^{-10}$	$5.33 \cdot 10^{-10}$	$5.45 \cdot 10^{-10}$
Time	46.18	46.75	45.18	45.35

B. RESULTS OF SMGSA'S APPLICATION TO COMPOSITE BENCHMARK TEST FUNCTIONS

Hybrid composite functions have been proposed in cases where the global fair value sought in the problem has same results in the middle of the search range, at the boundary, in the coordinate axis and at different variables and dimensions [59].

Table 7. Composite benchmark functions

Nr	Test Function	Dim	Range
CF1	$f_1, f_2, f_3, \dots, f_{10} = \text{Sphere function}$ $[\sigma_1, \sigma_2, \sigma_3, \dots, \sigma_{10}] = [1, 1, 1, \dots, 1]$ $[\lambda_1, \lambda_2, \lambda_3, \dots, \lambda_{10}] = [5/100, 5/100, 5/100, \dots, 5/100]$	10	[-5,5]
CF2	$f_1, f_2, f_3, \dots, f_{10} = \text{Griewank's function}$ $[\sigma_1, \sigma_2, \sigma_3, \dots, \sigma_{10}] = [1, 1, 1, \dots, 1]$ $[\lambda_1, \lambda_2, \lambda_3, \dots, \lambda_{10}] = [5/100, 5/100, 5/100, \dots, 5/100]$	10	[-5,5]
CF3	$f_1, f_2, f_3, \dots, f_{10} = \text{Griewank's function}$ $[\sigma_1, \sigma_2, \sigma_3, \dots, \sigma_{10}] = [1, 1, 1, \dots, 1]$ $[\lambda_1, \lambda_2, \lambda_3, \dots, \lambda_{10}] = [1, 1, 1, \dots, 1]$	10	[-5,5]
CF4	$f_1, f_2 = \text{Ackley's function}$ $f_3, f_4 = \text{Rastrigin's function}$ $f_5, f_6 = \text{Weierstrass function}$ $f_7, f_8 = \text{Griewank's function}$ $f_9, f_{10} = \text{Sphere function}$ $[\sigma_1, \sigma_2, \sigma_3, \dots, \sigma_{10}] = [1, 1, 1, \dots, 1]$ $[\lambda_1, \lambda_2, \lambda_3, \dots, \lambda_{10}] = [5/32, 5/32, 1, 1, 5/0.5, 5/0.5, 5/100, 5/100, 5/100, 5/100]$	10	[-5,5]
CF5	$f_1, f_2 = \text{Rastrigin's function}$ $f_3, f_4 = \text{Weierstrass function}$ $f_5, f_6 = \text{Griewank's function}$ $f_7, f_8 = \text{Ackley's function}$ $f_9, f_{10} = \text{Sphere function}$ $[\sigma_1, \sigma_2, \sigma_3, \dots, \sigma_{10}] = [1, 1, 1, \dots, 1]$ $[\lambda_1, \lambda_2, \lambda_3, \dots, \lambda_{10}] = [1/5, 1/5, 5/0.5, 5/0.5, 5/100, 5/100, 5/32, 5/32, 5/100, 5/100]$	10	[-5,5]
CF6	$f_1, f_2 = \text{Rastrigin's function}$ $f_3, f_4 = \text{Weierstrass function}$ $f_5, f_6 = \text{Griewank's function}$ $f_7, f_8 = \text{Ackley's function}$ $f_9, f_{10} = \text{Sphere function}$ $[\sigma_1, \sigma_2, \sigma_3, \dots, \sigma_{10}] = [0.1, 0.2, 0.3, 0.4, 0.5, 0.6, 0.7, 0.8, 0.9, 1]$ $[\lambda_1, \lambda_2, \lambda_3, \dots, \lambda_{10}] = [0.1 \times 1/5, 0.2 \times 1/5, 0.3 \times 5/0.5, 0.4 \times 5/0.5, 0.5 \times 5/100, 0.6 \times 5/100, 0.7 \times 5/32, 0.8 \times 5/32, 0.9 \times 5/100, 1 \times 5/100]$	10	[-5,5]

Composite benchmark functions have been carried out by applying merging, rotating, scrolling, and effecting operations to Single and multimodal test functions. With these group test functions, it is aimed to compare exploration and exploitation balance functions. Dragonfly Algorithm (DA), which is frequently mentioned recently together with well-known GA and PSO, has also been preferred to test and compare the performance in proposed SMGSA's composite benchmark functions. GA, PSO and DA data have been obtained from this new study [60]. SMGSA has been operated under 30 search agents and 500 cycles in the working environments same with DA.

SMGSA has produced the smallest value with respect to average best results and standard deviation values in 6 functions in Table 8. The SMGSA algorithm, when applied to composite test functions, has yielded positive results that could compete with the algorithms in the literature. SMGSA is able to be applied to complex problems in real life due to the high performance it exhibits.

500 cycles, 30 agent values and CF2 compound test function were selected to visually examine the performance of SMGSA. In Fig. 4 (a), the convergence rate of SMGSA is higher than that of GSA, the most appropriate value was reached at 100th iteration. It seems that it quickly reached the promising areas in the search space in Fig. 4 (b) and continued to search around the same area.

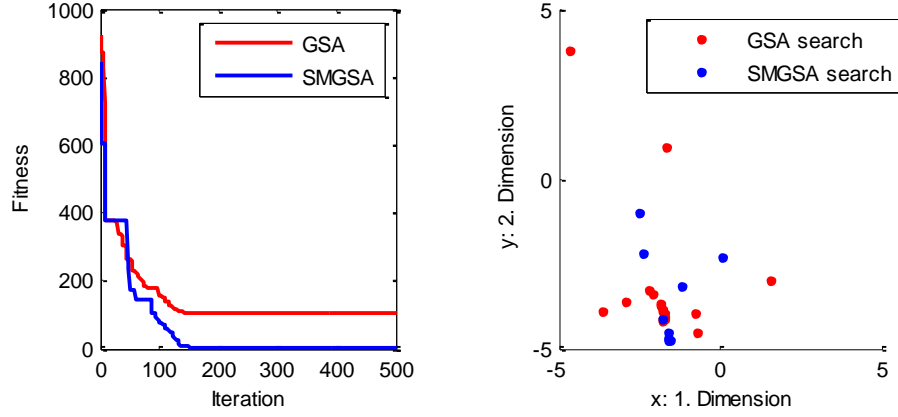


Figure 4. GSA and SMGSA's graphics and search results for CF2, (a) Best graphics from GSA and SMGSA on CF2, (b) Search history of the SMGSA and GSA for CF2

Table 8. Experimental results of composite benchmark functions

C.F.	GA [49]		PSO [49]		DA [49]		SMGSA	
	Ave	Std	Ave	Std	Ave	Std	Ave	Std
CF1	130.099	21.320	150	135.400	103.742	91.243	6.700	25.361
CF2	116.055	19.193	188.195	157.283	193.017	80.633	60.376	51.130.
CF3	383.918	36.605	263.094	187.135	458.296	165.372	169.198	93.531.
CF4	503.048	35.794	466.542	180.949	596.662	171.063	339.713	98.629
CF5	118.438	51.001	136.175	160.018	229.951	184.609	25.9611	68.487
CF6	544.101	13.301	741.634	206.729	679.588	199.401	594.731	172.97

C. APPLICATION OF IMAGE ENHANCEMENT WITH SMGSA

Image enhancement involves the reduction or elimination of distortions that may occur in an image, or the attempts to bring the image from its present state to a better state for a given purpose [61]. The basic tack in image enhancement is to generate a new intensity value for each corresponding pixel value in the image, by using transformation function after the intensity value of each pixel is taken in the input image. It was defined mathematically in Eq. (18).

$$g(i, j) = T[f(i, i)] \quad (18)$$

While $f(i, j)$ means input image, $g(i, j)$ means output image, T represents the transformation function that is applied to the pixel at the point (i, j) of the image in Eq.(18). The transformation function used in the study is named as local improvement method, and applies transformation on a pixel by considering the density distribution between neighboring pixels [25].

$$g(i, j) = \frac{k * D}{\varphi(i, j) + b} [f(i, j) - c * m(i, j)] + m(i, j)^a \quad (19)$$

In the equation, the expression $m(i, j)$ represents local mean value in a certain region, D represents global mean value calculated for the entire image and $\varphi(i, j)$ represents standard deviation value in $n \times n$ regional area. $a, b, c,$ and k in Eq (19) are parameter values and recommended SMGSA with the transformation function are used in order to optimize these 4 parameter values.

Objective evaluation criterion was used to measure the quality of the improved images upon finding the parameters of the transformation function with SMGSA. The objective function was proposed by combining three performance measures including entropy value of images, sum of edge densities and

number of edges [25]. It is also the most important feature that the quantity of edges of the improved image is higher and the edges have high density values when it is compared with the original image in the objective function expressed in Eq.(20) [29].

$$F(x) = \frac{\log(\log(E(I(x)))) \times n_{edge}(I(x)) \times H(I(x))}{M \times N} \quad (20)$$

In Eq.(20), $H(I(x))$ indicates the entropy value, $n_{edge}(I(x))$ indicates edge pixel number in the image and $E(I(x))$ indicates the sobel value of the image. M and N are the dimensions of the image.

The optimization of a, b, c and k parameter values of the transformation function used was carried out by SMGSA. The steps of the recommended method are as follows:

1. Randomly generate the values of a, b, c and k of the transformation function used,
2. Calculate the mean value of the input image (D), the standard deviation value $\varphi(i, j)$ within the 3×3 regional areas, and the mean value $m(i, j)$ and apply the transformation function to the input image,
3. Optimize a, b, c and k parameters using SMGSA,
4. Repeat the steps 2-3 until the improvement criterion is achieved.

Table 9. Objective evaluation results.

Name	Information	Met.	Best	Mean	SD	Time	Parameters			
Plane	Format:JPG Dimension:512x512 Bit depth:8	PSO	0.6659	0.6519	0.0564	0.1210	0.9498	0.4313	0.5105	0.5786
		DE	0.9668	0.9220	0.0353	0.1828	1.0593	0.3355	0.8903	0.5097
		DA	0.9090	0.7696	0.0986	0.1272	1.4000	0.2100	0.8248	0.5000
		GSA	0.9472	0.9296	0.0413	0.2437	1.4909	0.1892	0.7388	0.5872
		EVGSA	0.9647	0.9593	0.0075	0.2891	2.7709	0.1489	0.8986	0.3199
		SMGSA	0.9733	0.9698	0.0083	0.2794	1.3640	0.1044	0.7848	0.5122
Cameraman	Format:JPG Dimension:256x256 Bit depth:8	PSO	0.7716	0.7449	0.0626	0.0566	0.4066	0.2214	0.7101	0.6698
		DE	0.8747	0.6904	0.1312	0.0608	1.4936	0.2384	0.6919	0.5054
		DA	0.8622	0.7950	0.0411	0.0523	1.4298	0.3000	1.0000	0.6214
		GSA	0.8577	0.8413	0.0504	0.0754	1.4600	0.2242	0.8679	0.5449
		EVGSA	0.8855	0.8607	0.0438	0.0884	1.5944	0.1481	0.9257	0.3441
		SMGSA	0.9018	0.9006	0.0055	0.0871	1.4649	0.1338	0.9423	0.5058
Lena	Format:JPG Dimension:256x256 Bit depth:8	PSO	0.6614	0.6613	2.53.10 ⁻⁴	0.0449	0.1214	0.1569	0.7553	0.5148
		DE	0.8256	0.7986	0.0314	0.0551	1.4343	0.2517	0.8637	0.5903
		DA	0.8053	0.6994	0.0687	0.0450	1.2176	0.1449	0.8470	0.5748
		GSA	0.8199	0.8179	0.0026	0.0799	1.4723	0.1528	0.9514	0.5594
		EVGSA	0.8112	0.8042	0.0110	0.1010	2.5527	0.2052	0.9396	0.6621
		SMGSA	0.8278	0.8176	4.78.10⁻⁴	0.0929	1.4515	0.1974	0.9995	0.7272

The value ranges of a, b, c , and k parameters in the transformations function were determined as $a \in [0, 1.5]$, $b \in [0, 0.5]$, $c \in [0, 1]$ and $k \in [0.5, 1.5]$ by taking into consideration the previous studies [45]. In the proposed method, the following values were determined for SMGSA; $G_0=100$, $\alpha=20$, maximum iteration=20 and number of agents=20. Cameraman and Lena images in 256x256 jpeg format and Plane in 512x512 jpeg format were used to evaluate the effect of SMGSA's control parameter. Also, so as to test performance of SMGSA, PSO, Differential Evolution (DE), DA, GSA and Escape Velocity Gravitational Search Algorithm (EVGSA) heuristic optimization techniques are used in the study [29][62][60][34][14]. Best, Mean, Standard Deviation (SD) and Time results of the evaluation criterion obtained as a result of running the algorithm 30 times for different limit parameters, are given in Table 9.

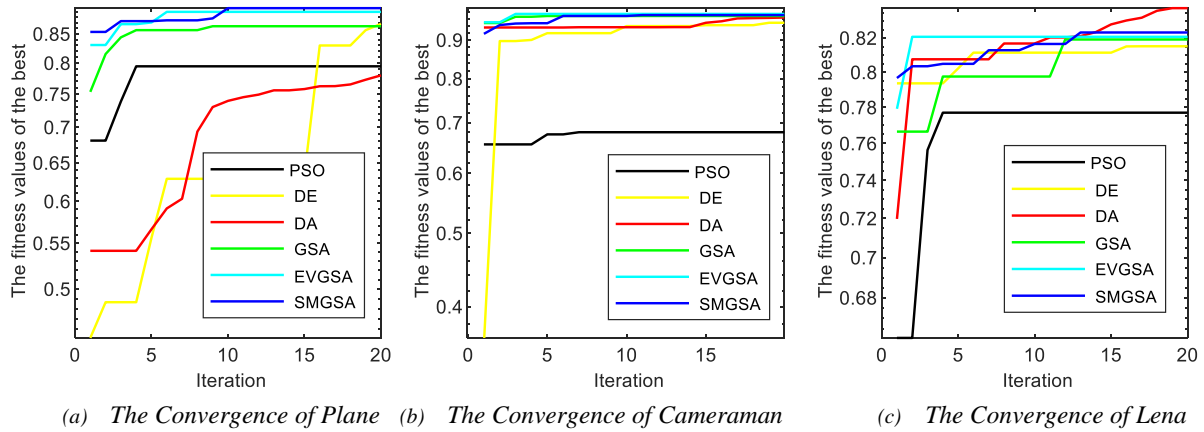


Figure 5. Plane and Cameraman convergence graphs using PSO, DE, DA, GSA, EVGSA and SMGSA optimization techniques

Applications were performed on MATLAB R2012b with Intel (R) Core (TM) i5-4200U CPU 2.30 GHz processor and 6 GB Ram. When the average running times are examined, it has been determined that the greatest disadvantage of SMGSA is the time spent because of the addition of best agent and chaotic calculations on standard GSA. It was seen that the highest success was obtained with SMGSA when PSO, DE, DA, GSA and EVGSA heuristic algorithms are compared according to the best fitness value results in Table 9. Best and Mean values are bigger than other GSA, PSO, DE and DA values. It is clearly seen that SMGSA has found best results as well as performed the search in the quickest manner.

Convergence diagram comparison of algorithms for control parameters from which my highest success is achieved in the table 9 is shown in Fig. 5. SMGSA show an efficient convergence in PSO, DE, DA and GSA convergence diagrams for Plane, Cameraman and Lena.

Measuring image quality is important for most of image processing applications. In this part, performance was inspected using objective evaluation methods of output image obtained with transformation function. Mean Square Error (MSE), Peak to Signal Noise Ratio (PSNR), Normalized Cross Correlation (NCC), Structural Content (SC), Average Difference (AD) and Structural Similarity Index Measurement (SSIM) have been used assessment methods. To obtain a better output image, PSNR, NCC and SSIM criteria must be high and MSE, SC and AD criteria must be low.

As a result of transformation function, excessive brightness, blur and deterioration in the images have been resolved with the proposed method. Moreover, natural and wide contrast enhancement was also obtained on the images. Results proving these sentences are provided in Table 10 for Plane image. Especially high value of PSNR, NCC and SSIM data in PSNR, NCC and SSIM functions shows the quality of output image.



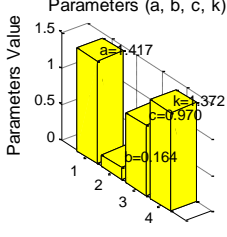
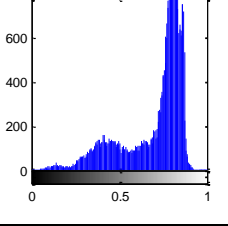
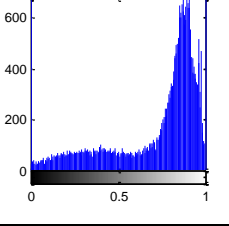
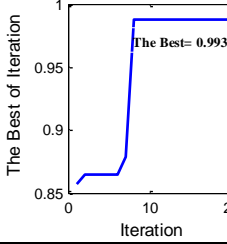


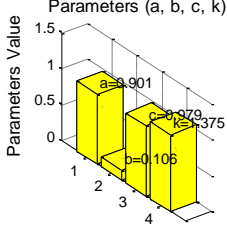
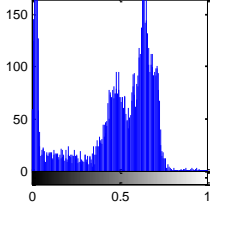
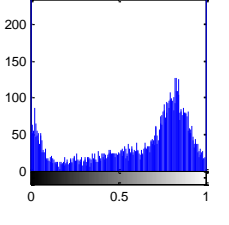
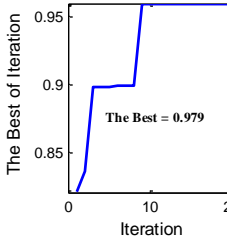


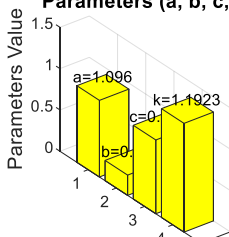
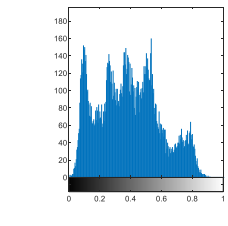
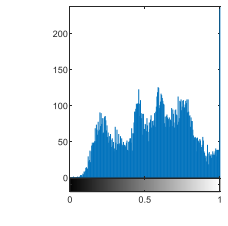
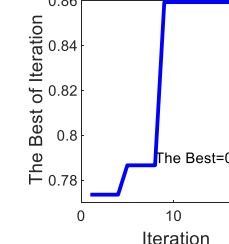
Plane			
	(a). Original Plane	(b). SMGSA output Plane	(c) Parameter bar graph of Plane
			
	(d). Original hist. of Plane	(e). SMGSA histogram of Plane	(f). Convergence graph of Plane
Cameraman			
	(g). Original Cameraman	(h). SMGSA output Cam.	(i) Bar graph of Cameraman
			
	(j). Original hist of Cameraman	(k). SMGSA his. of Cameraman	(l). Convergence graph of Cam.
Lena			
	(m). Original Lena	(n). SMGSA output Lena	(o) Parameter bar graph of Lena
			
	(p). Original histogram of Lena	(r). SMGSA histogram of Lena	(s). Convergence graph of Lena

Figure 6. SMGSA's image enhancement visual results and graphics

Table 10. Image quality visual results

Name	Met.	Entropy	Edge Pixels	Edge Intensity	MSE	PSNR	NCC	SC	AD	SSIM
Plane	PSO	1.3296	2917	1.07.10+4	3.37.10+4	2.8416	0,0057	2.93.10+4	178.15	0,0079
	DE	7.326	3232	2.63.10+4	3.39.10+4	2.8218	0.0034	8.59.10+4	178.58	0.0045
	DA	7.551	3314	3.13.10+4	3.39.10+4	2.8250	0.0037	6.93.10+4	178.51	0.0050
	GSA	6.7789	3300	3.19.10+4	3.38.10+4	2.8305	0.0044	5.14.10+4	178.40	0.0058
	EVGSA	7.5954	3354	3.75.10+4	3.39.10+4	2.8185	0.0030	4.04.10+4	178.65	0.0040
	SMGSA	6.9777	3356	3.45.10+4	3.38.10+4	2.8291	0,0042	3.05.10+4	178.43	0,0056
Cameraman	PSO	0	417	2.177.10+4	1.70.10+4	5.805	0.0090	3.45.10+3	114.03	0.1258
	DE	7.126	720	6.142.10+3	1.72.10+4	5.758	0.0034	8.27.10+4	115.54	0.0289
	DA	6.834	753	5.48.10+3	1.72.10+4	5.755	0.0031	1.02.10+5	115.57	0.0285
	GSA	6.961	694	5.68.10+3	1.72.10+4	5.756	0.0032	9.31.10+4	115.55	0.0287
	EVGSA	6.893	701	5.53.10+3	1.72.10+4	5.765	0.0031	1.07.10+5	115.57	0.0285
	SMGSA	6.835	693	5.33.10+3	1.72.10+4	5.754	0.0030	1.11.10+5	115.59	0.0283
Lena	PSO	0	528	4.48.10+3	1.21.10+4	7.285	0.0090	9.10.10+3	97.51	0.0184
	DE	6.487	548	4.71.10+3	1.23.10+4	7.221	0.0017	3.01.10+5	98.54	0.0023
	DA	7.180	617	6.74.10+3	1.23.10+4	7.230	0.0026	1.33.10+5	98.45	0.0032
	GSA	6.362	591	5.19.10+3	1.23.10+4	7.221	0.0017	3.01.10+5	98.54	0.0022
	EVGSA	6.569	607	5.47.10+3	1.23.10+4	7.223	0.0019	2.50.10+5	98.52	0.0024
	SMGSA	6.268	618	5.30.10+3	1.23.10+4	7.221	0.0016	3.11.10+5	98.55	0.0021

For Plane and Cameraman images, input and output images of the proposed SMGSA-based method, histograms, convergence graphs and bar graphs that show the transformation function parameters were included. When Fig. 6 is examined, the SMGSA method created brightness on these images, and an effective improvement was achieved. The success of this method was increased by optimizing the parameters of the transformation function used with SMGSA.

V. CONCLUSION

When the best result value doesn't change as the iterations progress in SMGSA, then are the agents tripped into the local minimum or in the bad search sector. In this case are the positions of the agents greatly changed by generating a chaotic shake on the gravitational constant. While generating the chaotic shake, the chaotic functions used are applied such to positively increase the gravitational constant. The speed was reduced by applying *Kworst* to the agent with the best value in order to cause SMGSA to gain precision search ability in the second stage of the search. Comparison tables are provided for each of the single and multimode test functions of the SMGSA algorithm. Examining the basic comparison tables, it is determined that the improvement was significant. In particular, it shows that the proposed algorithm makes a sensitive search with f_1 function $8.81.10^{-23}$ and f_6 function $3.80.10^{-24}$ values. While the zero hypothesis is rejected at total 7 functions, according to the Wilcoxon signed-rant test results of the SMGSA, the zero-hypothesis realized at the other functions. It will be seen that the GSA and SMGSA results are all same or very close to each other at these functions with realized zero hypothesis. SMGSA has accomplished the exploration and exploitation actions in a balance in the search space change. Also, SMGSA can be applied to complex problems in real life due to the high performance it has achieved.

SMGSA was applied to the transformation function among image enhancement techniques which are engineering applications. The success of this method has been increased by optimizing the parameters of the transformation function used. SMGSA has the best fitness values, such as Plane 0.9733, Cameraman 0.9018 and Lena 0.8278, and it has performed an effective image enhancement process by adjusting the natural contrast and brightness on the images. Compared to other algorithms used in the study, the biggest disadvantage is the high processing time. Especially, finding the best agent according to GSA, reducing the speed of the best agent and creating chaotic shakes to get rid of the local minimum are the agents that increase the process time.

VI. REFERENCES

- [1] C. R. Reeves, *Modern heuristic techniques for combinatorial problems*, John Wiley & Sons, Inc, 1993.
- [2] T. Cura, *Modern heuristic techniques and applications*, Papatya, Istanbul, 2008.
- [3] S. Salhi, *Heuristic search methods*, Mahwah, NJ: Erlbaum, 1998.
- [4] A. R. Bhowmik, A. K. Chakraborty, "Solution of optimal power flow using nondominated sorting multi objective gravitational search algorithm," *Electrical Power and Energy Systems*, vol. 62, pp. 323-334, 2014.
- [5] C. Li, H. Li, and P. Kou, "Piecewise function based gravitational search algorithm and its application on parameter identification of AVR system," *Neurocomputing*, vol. 124, pp. 139-148, 2013.
- [6] J. Vijaya Kumar, D. M. Vinod Kumar, and K. Edukondalu, "Strategic bidding using fuzzy adaptive gravitational search algorithm in a pool based electricity market," *Applied Soft Computing*, vol. 13, pp. 2445-2455, 2012.
- [7] H. Askari, S. H. Zahiri, "Intelligent gravitational search algorithm for optimum design of fuzzy classifier," 2nd International eConference on Computer and Knowledge Engineering, Mashhad, Iran, 2012, pp. 98-104.
- [8] Y. Sun, Z. Tang, J. Lu, P. Du, "Optimal Multilevel Thresholding using Improved Gravitational Search Algorithm for Image Segmentation," In *Mechatronic Sciences, Electric Engineering and Computer (MEC)*, Proceedings 2013 International Conference on IEEE, Shenyang, China, 2013, pp. 1487-1490.
- [9] A. Sombra, F. Valdez, P. Melin, "Castillo O. A new gravitational search algorithm using fuzzy logic to parameter adaptation," In *Evolutionary Computation (CEC) 2013 IEEE Congress on IEEE*, Cancun, Mexico, 2013, pp. 1068-1074.
- [10] F. Saeidi-Khabisi, E. Rashedi, "Fuzzy Gravitational Search Algorithm," 2nd International eConference on Computer and Knowledge Engineering, Mashhad, Iran, 2012, pp. 156-160.
- [11] G. Sun, A. Zhang, Y. Yao, Z. Wang, "A novel hybrid algorithm of gravitational search algorithm with genetic algorithm for multi-level thresholding," *Applied Soft Computing*, vol. 46, pp. 703-730, 2016.
- [12] C. Li, L. Chang, Z. Huang, Y. Liu, N. Zhang, "Parameter identification of a nonlinear model of hydraulic turbine governing system with an elastic water hammer based on a modified gravitational search algorithm," *Engineering Applications of Artificial Intelligence*, vol. 50, pp. 177-191, 2016.
- [13] G. Sun, P. Ma, J. Ren, A. Zhang, X. Jia, "A stability constrained adaptive alpha for gravitational search algorithm," *Knowledge-Based Systems*, vol. 139, pp. 200-213, 2018.
- [14] U. Güvenç, F. Katircioğlu, "Escape velocity: a new operator for gravitational search algorithm," *Neural Computing and Applications*, vol. 31, no. 1, pp. 27-42, 2019.
- [15] K. Kang, C. Bae, H. W. F. Yeung, Y. Y. Chung, "A hybrid gravitational search algorithm with swarm intelligence and deep convolutional feature for object tracking optimization," *Applied Soft Computing*, vol. 66, pp. 319-329, 2018.

- [16] R. J. Schalkoff, “*Digital image processing and computer vision*,” New York: Wiley, 1989.
- [17] J. C. Russ, F. B. Neal, “*The image processing handbook*,” 7th ed., CRC press, 2017.
- [18] Y. T. Kim, “Contrast enhancement using brightness preserving bi-histogram equalization,” *IEEE transactions on Consumer Electronics*, vol. 43, no. 1, pp. 1-8, 1997.
- [19] S. D. Chen, A. R. Ramli, “Contrast enhancement using recursive mean-separate histogram equalization for scalable brightness preservation,” *IEEE Transactions on consumer Electronics*, vol. 49, no. 4, pp. 1301-1309, 2003.
- [20] K. S. Sim, C. P. Tso, Y. Y. Tan, “Recursive sub-image histogram equalization applied to gray scale images,” *Pattern Recognition Letters*, vol. 28, no. 10, pp. 1209-1221, 2007.
- [21] G. Tanaka, N. Suetake, E. Uchino, “Image enhancement based on multiple parametric sigmoid functions,” In *Intelligent Signal Processing and Communication Systems, 2007 ISPACS, 2007*, pp. 108-111.
- [22] P. Kannan, S. Deepa, R. Ramakrishnan, “Contrast enhancement of sports images using modified sigmoid mapping function,” In *Communication Control and Computing Technologies (ICCCCT), 2010*, pp. 651-656.
- [23] H. K. Verma, S. Pal, “Modified Sigmoid Function Based Gray Scale Image Contrast Enhancement Using Particle Swarm Optimization,” *Journal of The Institution of Engineers (India): Series B*, vol. 97, no. 2, pp. 243-251, 2016.
- [24] C. Munteanu, A. Rosa, “Towards automatic image enhancement using genetic algorithms,” In *Evolutionary Computation, Proceedings of the 2000 Congress on 2, 2000*, pp. 1535-1542.
- [25] A. Gorai, A. Ghosh, “Gray-level image enhancement by particle swarm optimization,” In *Nature & Biologically Inspired Computing*, pp. 72-77, 2009.
- [26] W. Zhao, “Adaptive image enhancement based on gravitational search algorithm,” *Procedia Engineering*, vol. 15, pp. 3288-3292, 2011.
- [27] S. Agrawal, R. Panda, “An efficient algorithm for gray level image enhancement using cuckoo search,” In *International Conference on Swarm, Evolutionary, and Memetic Computing*, pp. 82-89, 2012.
- [28] P. P. Sarangi, B. S. P. Mishra, B. Majhi, S. Dehuri, “Gray-level image enhancement using differential evolution optimization algorithm,” In *Signal Processing and Integrated Networks (SPIN), 2014 International Conference, 2014*, pp. 95-100.
- [29] K. Murali, T. Jayabarathi, “Automated image enhancement using Grey-wolf optimizer algorithm,” *J Multidiscip Sci Technol*, vol. 7, pp. 77-84, 2016.
- [30] A. M. Nickfarjam, H. Ebrahimpour-Komleh, “Multi-resolution gray-level image enhancement using particle swarm optimization,” *Applied Intelligence*, vol. 47, no. 4, pp. 1132-1143, 2017.
- [31] K. G. Dhal, S. Ray, A. Das, S. Das, “A survey on nature-inspired optimization algorithms and their application in image enhancement domain,” *Archives of Computational Methods in Engineering*, vol. 26, no. 5, pp. 1607-1638, 2019.

- [32] H. Singh, A. Kumar, L. K. Balyan, G. K. Singh, "A novel optimally weighted framework of piecewise gamma corrected fractional order masking for satellite image enhancement," *Computers & Electrical Engineering*, vol. 75, pp. 245-261, 2019.
- [33] P. Kandhway, A. K. Bhandari, A. Singh, "A novel reformed histogram equalization based medical image contrast enhancement using krill herd optimization," *Biomedical Signal Processing and Control*, vol. 56, pp. 101677, 2020.
- [34] E. Rashedi, H. Nezamabadi-Pour, S. Saryazdi, "GSA: a gravitational search algorithm," *Information sciences*, vol. 179, no. 13, pp. 2232-2248, 2009.
- [35] S. Sarafrazi, H. Nezamabadi-Pour, S. Saryazdi, "Disruption: a new operator in gravitational search algorithm," *Scientia Iranica*, vol. 18, no. 3, pp. 539-548, 2011.
- [36] X. Han, X. A. Chang, "Chaotic digital secure communication based on a modified gravitational search algorithm filter," *Information Sciences*, vol. 208, pp. 14-27, 2012.
- [37] S. Mirjalili, S. Z. M. Hashim, "A new hybrid PSO-GSA algorithm for function optimization," In *Computer and information application (ICCIA)*, 2010 international conference on IEEE, Tianjin, China, pp. 374-377, 2010.
- [38] B. Gu, F. Pan, "Modified gravitational search algorithm with particle memory ability and its application," *International Journal of Innovative Computing, Information and Control*, vol. 9, no. 11, pp. 4531-4544, 2013.
- [39] F. Katircioglu, U. Güvenc, "Sarsıntı Operatörü: Yerçekimi Arama Algoritması İçin Yeni Bir Operatör," *Akıllı Sistemlerde Yenilikler ve Uygulamaları Sempozyumu ASYU*, 2016, pp. 132-137.
- [40] F. Katircioglu, "Improving a new operators for Gravitation Search Algorithm," *Doctoral Thesis, Graduate School of Natural and Applied Sciences, Department of Electrical-Electronic and Computer Engineer, Duzce University, Duzce, Turkey*, 2016.
- [41] S. Mirjalili, A. H. Gandomi, "Chaotic gravitational constants for the gravitational search algorithm," *Applied Soft Computing*, vol. 53, pp. 407-419, 2017.
- [42] G. Wang, S. He, "A quantitative study on detection and estimation of weak signals by using chaotic Duffing oscillators," *Circuits and Systems I: Fundamental Theory and Applications, IEEE Transactions*, vol. 50, no. 7, pp. 945-953, 2003.
- [43] E. N. Lorenz, "Deterministic nonperiodic flow," *Journal of the atmospheric sciences*, vol. 20, no. 2, pp. 130-141, 1963.
- [44] E. Ott, C. Grebogi, J. A. Yorke, "Controlling chaos," *Physical review letters*, vol. 64, no. 11, pp. 1196, 1990.
- [45] T. L. Liao, S. H. Tsai, "Adaptive synchronization of chaotic systems and its application to secure communications," *Chaos, Solitons & Fractals*, vol. 11, no. 9, pp. 1387-1396, 2000.
- [46] S. Haykin, B. Li, "Detection of signals in chaos," *Proceedings of the IEEE*, vol. 83, no. 1, pp. 95-122, 1995.
- [47] L. Yang, T. L. Chen, "Application of chaos in genetic algorithms. *Commun Theor Phys*, vol. 38, no. 1, pp. 168-172, 2002.

- [48] G. Zhenyu, L. Jia, X. Gao, J. Liu, F. Wu, "Self-adaptive chaos differential evolution," *Advances in natural computation*, vol. 4221, pp. 972-975, 2006.
- [49] D. Simon, "Biogeography-based optimization," *IEEE Trans Evol Comput*, vol. 12, pp. 702-713, 2008.
- [50] D. Du, D. Simon, M. Ergezer, "Biogeography-based optimization combined with evolutionary strategy and immigration refusal," *IEEE international conference on systems*, 2009, pp. 997-1002.
- [51] U. Güvenc, F. Katircioğlu, "En iyi ajana özel davranış: Geliştirilmiş yerçekimi arama algoritması," *Ecjse Journal of Science and Engineering*, vol. 3, no. 1, pp. 143-153, 2016.
- [52] P. N. Suganthan, N. Hansen, J. J. Liang, K. Deb, Y. P. Chen, A. Auger, S. Tiwari, "Problem definitions and evaluation criteria for the CEC 2005 special session on real-parameter optimization." KanGAL report, Singapore, 2005.
- [53] R. L. Haupt, S. E. Haupt, *Practical genetic algorithms*. John Wiley & Sons, Pennsylvania, 2004.
- [54] H. C. Tsai, Y. Y. Tyan, Y. W. Wu, Y. H. Lin, "Gravitational particle swarm," *Applied Mathematics and Computation*, vol. 219, no. 17, pp. 9106-9117, 2013.
- [55] X. Han, L. Quan, X. Xiong, B. Wu, "Diversity enhanced and local search accelerated gravitational search algorithm for data fitting with B-splines," *Engineering with Computers*, vol. 31, no. 2, pp. 215-236, 2015.
- [56] S. Garcia, "A study on the use of non-parametric tests for analyzing the evolutionary algorithms' behaviour: a case study on the cec'2005 special on real parameter optimization," *Journal of Heuristics*, vol. 15, no. 6, pp. 617-644, 2009.
- [57] F. Wilcoxon, "Individual comparisons by ranking methods," *Biometrics*, vol. 1, no. 6, pp. 80-83, 1945.
- [58] A. Zhang, "A hybrid genetic algorithm and gravitational search algorithm for global optimization," *Neural Network World*, vol. 25, no. 3, pp. 53-73, 2015.
- [59] J. J. Liang, P. N. Suganthan, K. Deb, "Novel composition test functions for numerical global optimization," In *Proceedings 2005 IEEE Swarm Intelligence Symposium, SIS, 2005*, pp. 68-75.
- [60] S. Mirjalili, "Dragonfly algorithm: a new meta-heuristic optimization technique for solving single-objective, discrete, and multi-objective problems," *Neural Computing and Applications*, vol. 27, no. 4, pp. 1053-1073, 2016.
- [61] S. Öztürk, N. Öztürk, "Improvement of Image Enhancement Method Using Artificial Bee Colony Algorithm," *Gazi Üniversitesi Fen Bilimleri Dergisi Part C: Tasarım ve Teknoloji*, vol. 4, no. 4, pp. 173-183, 2016.
- [62] L. Dos Santos Coelho, J. G. Sauer, M. Rudek, "Differential evolution optimization combined with chaotic sequences for image contrast enhancement," *Chaos, solitons & fractals*, vol. 42, no. 1, pp. 522-529, 2009.